Title
MOMENTUM TRANSFER IN HEAVY-ION-INDUCED FISSION

Authors
Sikkeland, Torbjorn
Haines, Eldon L.
Viola, Victor E.

Publication Date
1961-07-01

UCRL -9751

UNIVERSITY OF CALIFORNIA

Ernest O. Lawrence Radiation Laboratory

BERKELEY, CALIFORNIA

DISCLAIMER

UCRL-9751

UNIVERSITY OF CALIFORNIA

Lawrence Radiation Laboratory
Berkeley, California

Contract No. W-7405-eng-48

MOMENTUM TRANSFER IN HEAVY-ION-INDUCED FISSION

Torbjørn Sikkeland, Eldon L. Haines, and Victor E. Viola, Jr.

July 1961

MOMENTUM TRANSFER IN HEAVY-ION-INDUCED FISSION

Torbjørn Sikkeland, Eldon L. Haines, and Victor E. Viola, Jr.

University of California
Lawrence Radiation Laboratory
Berkeley, California

July 1961

ABSTRACT

The forward linear momentum transfer in reactions leading to fission between heavy ions such as C^{12}, N^{14}, O^{16}, and Ne^{20} and the target nuclei Ho, Au, Bi, and U^{238} has been investigated by measuring the angular correlation between the fragments. The experimental values for the most probable parameters for center-of-mass transformation for these systems are compared with calculated values. For all the systems, the dominant reaction involves a full momentum transfer by the heavy ion to the fissioning nucleus. For systems such as Au + Ne^{20} and Bi + Ne^{20}, contributions from reactions with incomplete momentum deposition are observed. For U^{238} an appreciable admixture of such reactions occurs for all ions at the highest bombarding energies. Possible reaction mechanisms leading to fission are suggested. A brief discussion of the method and its application is given.

MOMENTUM TRANSFER IN HEAVY-ION-INDUCED FISSION *

Torbjørn Sikkeland, Eldon L. Haines, and Victor E. Viola, Jr.

University of California
Lawrence Radiation Laboratory
Berkeley, California

July 1961

INTRODUCTION

In any model for a nuclear reaction, linear momentum must be conserved. It is therefore of importance to be able to perform a momentum analysis experimentally.

In the study of reactions that lead to fission, angular-distribution measurements of the fragments furnish average values for the forward momentum transferred by the ion to the fissioning nucleus. The distribution in the laboratory system is transformed to the coordinate system of the fissioning nucleus (from now on called the c.m. system) by use of the parameter x^2, defined as

$$x^2 = (v_{fN}/v_{ff})^2. \qquad (1)$$

Here v_{fN} is the velocity component of the fissioning nucleus along the beam axis, and v_{ff} is the velocity of the fission fragment in the c.m. system. This transformation yields mean values of x^2, x_m^2.[1,2,3] The same value is obtained by measuring the median range of fission fragments in emulsion vs laboratory angle.[4] Alexander and Gazdik measured ranges of fragments in aluminum in the forward and backward directions, from which average values for v_{fN} could be deduced.[5]

By measuring the most probable fragment kinetic energy in the laboratory system, E_L, as a function of angle one can evaluate x_{mp}^2, the most probable value for x^2.[2] The values obtained with these methods are

* This work was done under the auspices of the U. S. Atomic Energy Comission.

not very accurate however. They are insensitive for the detection of components in a mixture of reactions involving varying degrees of momentum transfer.

Indications for reactions with incomplete momentum deposition, from now on called non-compound-nucleus (NCN) reactions, have been observed for the system $U^{238} + C^{12}$.[2] For that system, any reaction depositing more than 5 Mev excitation energy leads in most cases, to fission. For lighter elements, the fission thresholds are higher and fission occurs only for compound-nucleus (CN) reactions in which the heavy ion amalgamates with the target nucleus, or other reactions in which large excitations are produced. The investigation reported here was undertaken with a new method which was expected to be more sensitive and more direct in the analysis of the x^2 values.

The method consists of measuring the fragment-fragment coincidence rate as a function of the angular positions ψ_1 and ψ_2 of the fragments relative to the beam axis. With the detectors placed on opposite sides and in the plane of the beam axis, the conditions for coincidence are

$$\tan \psi_1 = \sin \theta_{c.m.} / (x_1 + \cos \theta_{c.m.}), \tag{2}$$

$$\tan \psi_2 = \sin \theta_{c.m.} / (x_2 - \cos \theta_{c.m.}). \tag{3}$$

Here x is as defined before and $\theta_{c.m.}$ is the c.m. angle. For one value of v_{fN} conditions Eqs. (2) and (3) are fulfilled for a variety of (x_1, x_2) values because of the wide spread in the velocity of the fragments, giving coincidences over a range of ψ_1 and ψ_2. For high-energy fission, symmetric division is the most probable mode. Because of conservation of momentum the fragment velocities are equal, therefore a maximum coincidence rate is expected for $x_1 = x_2 = x_{mp}$. The most probable x^2 value, x_{mp}^2, can thus be determined. If several v_{fN} values are present, the curve is expected to exhibit more than one peak.

EXPERIMENTAL PROCEDURE

Heavy-ion beams were obtained from the Berkeley heavy-ion linear accelerator (Hilac), which accelerates ions to 10.4±0.2 Mev/nucleon.[6] The beam was deflected through 15 deg by a bending magnet before reaching the fission and scatter chamber, which is shown in Fig. 1. Lower energies were obtained by inserting weighed aluminum foils into the beam path. Measured range-energy curves for aluminum were used to estimate the resulting energy.[7]

Before striking the target, the beam passed through two 1.5 x 6-mm collimators 25 in. apart. The last collimator was 2 1/4 in. from the target. Beam particles were collected in a 3-in.-wide Faraday cup at the rear of the chamber. In front of the cup was a permanent magnet which prevented electrons from entering or leaving the cup.

Targets were either self-supporting or supported by 100-μg/cm^2 thick nickel films. Target thicknesses were generally around 200 μg/cm^2. The target was mounted in the center of the tank and its orientation with respect to the beam could be changed.

The detectors used were crystals covered with Au, about 50 μg/cm^2 thick.[8] They were mounted on arms which could be moved independently of each other around the center of the tank in all directions except for approximately 10 degrees in the backward direction. The distances of the detectors from the target and their angular positions could be adjusted while the tank was under vacuum. In front of the detectors was a collimating system which defined the geometry. The angular position of each detector was determined to ± 1/4 deg by counting elastically scattered heavy ions.

The electronic system (Fig. 2) consisted of two linear amplifier systems and a fast-coincidence system. The "slow" pulse (1μsec width) from each crystal was passed through a preamplifier in the bombardment area and then to a doubly differentiating linear amplifier in the counting area.

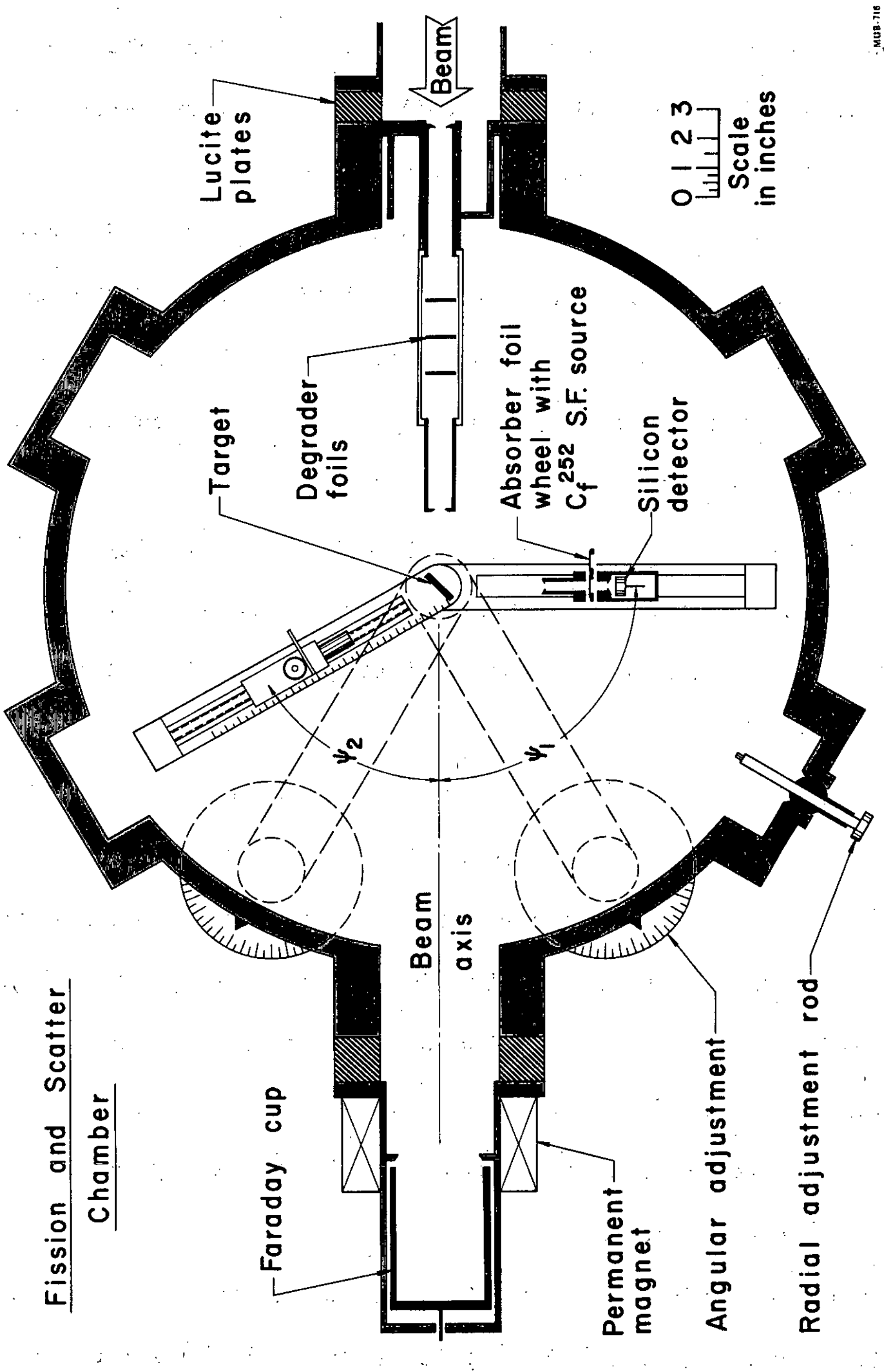

Fig. 1. Schematic diagram of the fission and scatter chamber.

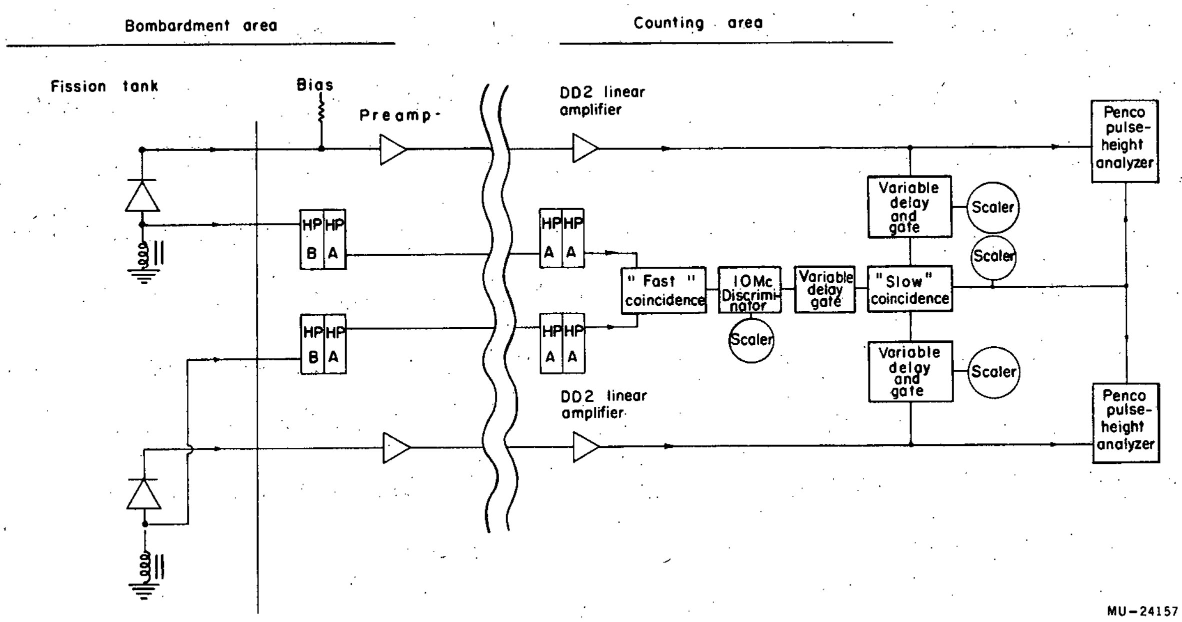

Fig. 2. Electronic system used in the angular correlation experiments.

The amplified signals were transmitted to variable delay and gate units and then into individual scalers and a transistorized coincidence unit. The "fast" pulse (4 n sec width) from each crystal was passed through two distributed amplifiers in the bombardment area and then to the counting area by way of high-impedance cables. After further amplification, the pulses were fed through a transistorized fast-coincidence unit. The output pulse from this unit was led through a 10-megacycle discriminator-scaler and a variable-delay and gate unit into the coincidence unit used by the linear system. Thus three-way coincidence was demanded between two linear pulses and a fast coincidence pulse. The output pulse of this coincidence unit drove a scaler and was used as a gate pulse for two Penco 100-channel pulse-height analyzers to analyze the linear pulses. The use of fast coincidence reduced the accidentals to a negligible rate, even with one detector at a forward angle where large numbers of beam particles were detected.

ENERGY MEASUREMENTS

In order to interpret the results, determination of the most probable kinetic energy of the fragments was necessary. Previous results have shown a defect in the energy spectrum of the fragments from the spontaneous fission of Cf^{252} as observed with a silicon detector.[2] An attempt was therefore made to obtain a more reliable curve of energy vs pulse height for such a detector. For that purpose, the most probable laboratory-system kinetic energy, E_L, of the fragments from fission induced by heavy ions was used as a convenient calibration source. E_L varies with angle according to the equation

$$E_L = E_{c.m.}(1+x_{mp}^2+2x_{mp}\cos\theta_{c.m.}). \qquad (4)$$

The $\theta_{c.m.}$, the c.m. angle, is related to the lab angle ψ by eq. (2); $E_{c.m.}$ is the most probable kinetic energy in the c.m. system after the prompt neutron emission, and is to a good approximation a constant independent of $\theta_{c.m.}$. Values for x_{mp}^2, the most probable x^2 value, for several systems are measured directly and to a high accuracy in this investigation, as is shown in the next section. We decided to use the system Au+166-Mev O^{16} for calibration, since this gives a wide range of E_L. The x_{mp}^2 value as given in Table I is 0.074±0.002.

The variation of E_L with ψ is known by determining the angle at which the pulse height is equal to the most probable pulse height produced by the light fragments from a Cf^{252} source. At that position E_L = 103 Mev, which is the most probable kinetic energy (corrected for energy loss due to evaporated neutrons) of the light-fragment group as determined with the time-of-flight technique.[9] This peak was chosen because the values for the most probable mass, A_{ff}, from the two sources are comparable (110 for Cf^{252} and 100 for Au + 166-Mev O^{16}). In both cases the fragments suffer the same energy degradation in the Au "window" of the crystal. The energy degradation in the 200-μg/cm^2 Au target was determined experimentally by placing the target surface first parallel and then at 45 deg to the surface of the crystal. The correction to "zero thickness" was found to be about 1 Mev.

The heavy-fragment group from Cf^{252} has a most probable mass of 140 and a kinetic energy of 79 Mev. It is interesting to note that a fragment with mass 100 and the same energy gives a higher pulse height. At this energy, there appears to be a "mass defect" of approximately 70 kev/nucleon. From Table I it is seen that the fragments we are dealing with have A_{ff} ranging from 100 to 120 amu and the mass-defect correction should therefore be comparable. The quantity in which we are interested is $E_{c.m.}$. Because x_{mp}^2 is determined experimentally by another method, $E_{c.m.}$ is found by measuring E_L for one position of the detector. To avoid the possibility that the "mass defect" might vary with energy, a position was chosen which

Table I.

Measured and calculated properties of each fissioning system studied in this work. $W_{1/2}$ is the angular width at half maximum for the angular correlation. Other symbols are defined in the text.

Heavy ion	Target	Heavy-ion energy (Mev)	ψ_1 (deg)	ψ_{2mp} (deg)	$W_{1/2}$ (deg)	X_{mp}^2	NCN (%)	$E_{c.m.}$ (Mev)	A_{ff} (amu)	$\overline{X}_{CN}^2$
C^{12}	Ho^{165}	125	90	61.6	6.5	0.068	0	63[d]	82.2	0.062
	Au^{197}	125	90	66.8	7.3	0.044	0	73[a]	98.5	0.046
	Bi^{209}	125	90	68.0	6.6	0.039	0	78[d]	105.3	0.041
	U^{238}	125	90	70.2	7.0	0.031	11.9%	91[c]	117.6	0.031
	U^{238}	93.7	90	72.4	6.8	0.025	1.8%	91[c]	119.3	0.024
	U^{238}	74.8	90	74.3	6.2	0.019	0	91[c]	120.4	0.019
N^{14}	Au^{197}	145	90	64.4	7.9	0.054	~0	74[d]	98.4	0.061
	Bi^{209}	145	90	65.9	7.7	0.052	~0	79[d]	105.2	0.055
	U^{238}	145	90	68.2	7.1	0.039	16.9%	92[d]	117.4	0.041
	U^{238}	145	40	122.5	8.0	0.042	8.7%	92[d]	117.4	0.041
	U^{238}	103	90	71.2	6.7	0.028	4.8%	92[d]	119.1	0.028
O^{16}	Ho^{165}	166	90	54.7	7.8	0.111	0	65[a]	81.8	0.102
	Au^{197}	166	90	60.5	7.8	0.074	~1%	75[b]	99.0	0.077
	Bi^{209}	166	90	62.1	6.2	0.066	~0	80[b]	104.8	0.069
	U^{238}	166	90	64.6	7.1	0.053	15.7%	93[a]	117.8	0.052
	U^{238}	166	40	120.4	8.6	0.052	8.4%	93[a]	117.8	0.052
	U^{238}	140	90	66.6	7.6	0.045	10.2%	93[a]	119.3	0.045
	U^{238}	110	90	68.8	6.2	0.036	3.2%	93[a]	121.0	0.035
Ne^{20}	Au^{197}	207	90	55.3	9.5	0.107	5.1%	77[d]	99.8	0.111
	Bi^{209}	207	90	57.0	9.0	0.095	8.6%	82[d]	106.1	0.095
	U^{238}	207	90	60.8	7.9	0.072	16.4%	95[d]	118.3	0.078

[a] This work
[b] Ref 10
[c] Ref 2
[d] Estimated

yielded an E_L close to 79 Mev. The over-all error in the value for $E_{c.m.}$ obtained by this method is believed to be less than 4%.

RESULTS AND DISCUSSION

In the coincidence measurements, one of the detectors was placed at a fixed position, ψ_1, while the angle of the other detector, ψ_2, was varied. In most of the experiments ψ_1 was set at 90 deg. In a few cases $\psi_1 = 40$ deg was also chosen in order to investigate any angular variation. The angular resolution was around 2 deg.

Curves for some of the systems investigated are reproduced in Figs. 3 through 12. Generally the curves can be divided into two groups. In the first group the curves are characterized by a symmetric peak with a half-width around 6 to 9 deg. Corrected for angular resolution, this corresponds to an intrinsic half-width of 5 to 8 deg. To this group belong the Ho, Au, and Bi targets and also the system U^{238} + 73-Mev C^{12} ions. Figure 3 shows the system Au + C^{12} which is typical for this group. In regard to the total coincidence curve, the appearance of a symmetric peak is expected in a case with specific momentum transfer followed by symmetric fission. Coincidence curves of the other group are characterized by an asymmetric peak. Some typical curves are shown in Figs. 4 through 12. In this group, we see that for the same bombarding energy, the peak becomes more distorted as the masses of the target and projectile increase. The distortion is toward higher angles, which correspond to lower x^2 values.

We first consider the main peak. At the peak, as we have discussed before, $x_1 = x_2 = x_{mp}$. Values for x_{mp}^2 for Groups I and II are given in Table I. The uncertainty of the values is of the order of ± 3%, corresponding to a ± 1/4-deg uncertainty in the position of the peak. As is seen from Table I, x_{mp}^2 does not seem to vary with angle.

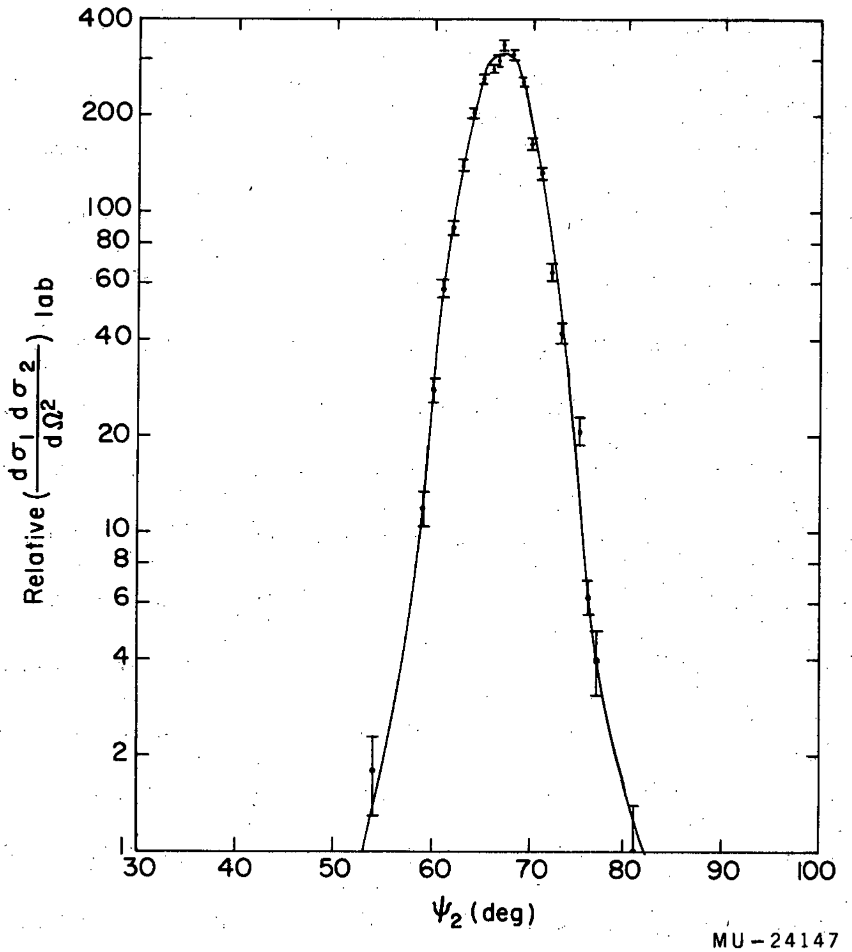

Fig. 3. Fission-fragment angular correlation for the system 125-Mev $C^{12}+Au^{197}$. ψ_1 at 90 deg.

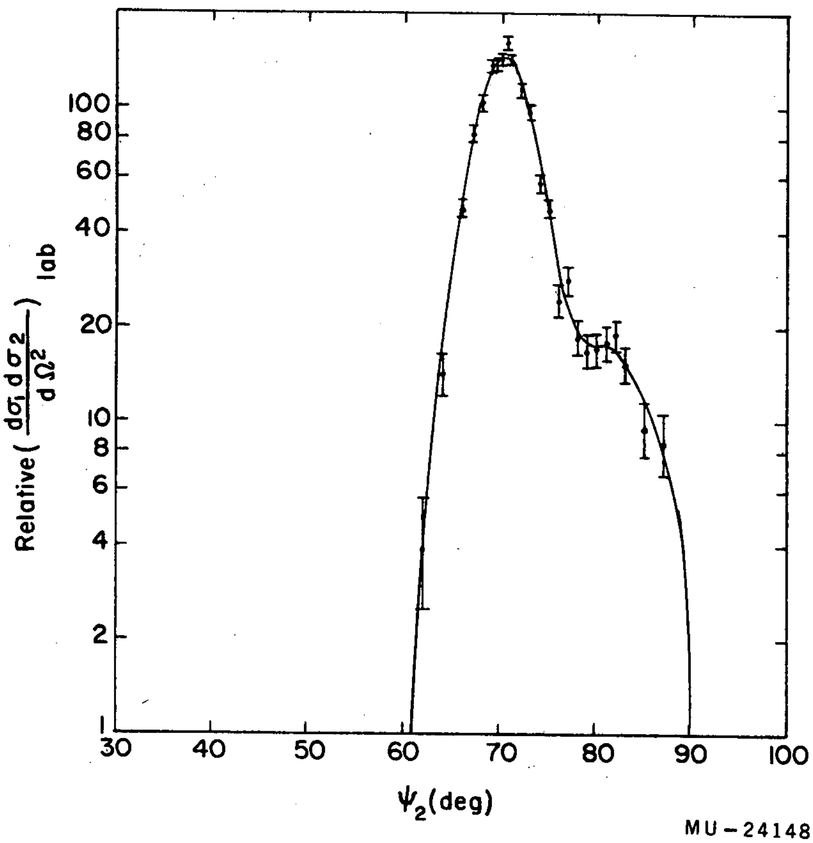

Fig. 4. Fission fragment angular correlation for the system 125-Mev $C^{12}+U^{238}$. ψ_1 at 90 deg.

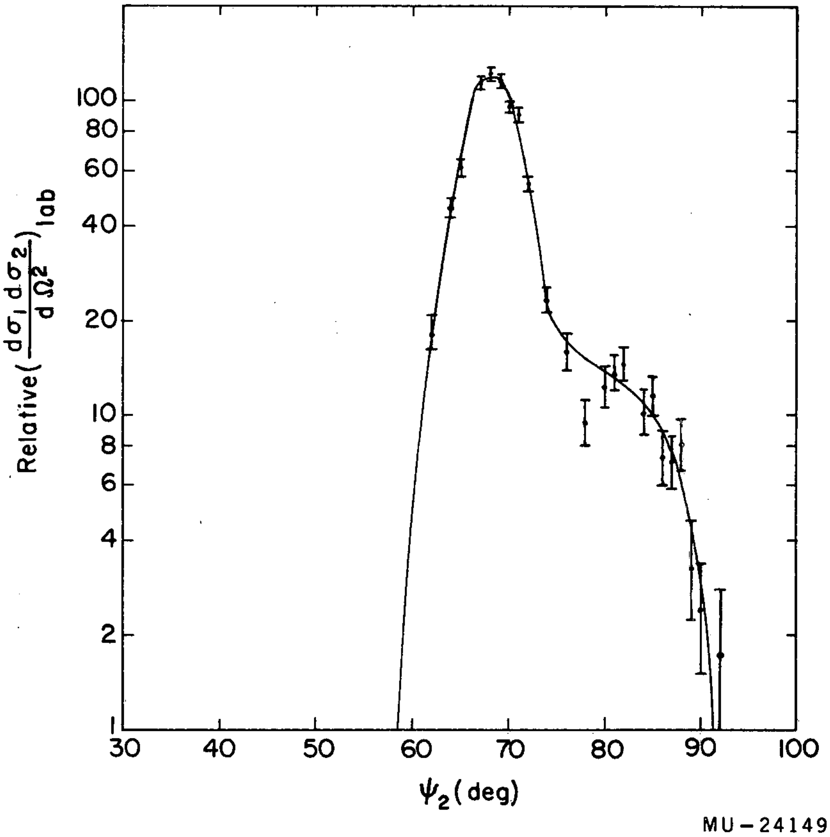

Fig. 5. Fission-fragment angular correlation for the system 145-Mev $N^{14}+U^{238}$. ψ_1 at 90 deg.

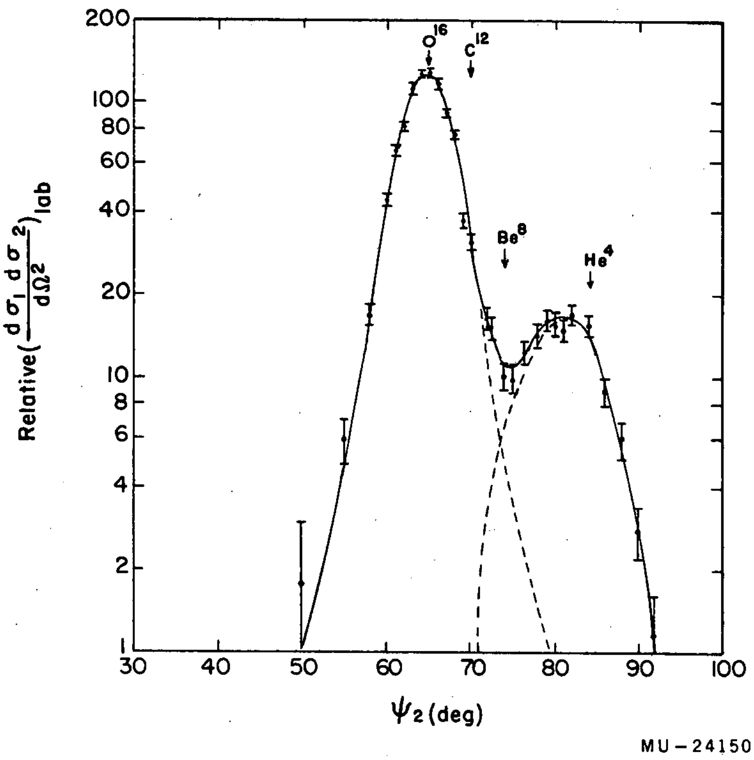

Fig. 6. Fissión-fragment angular correlation for the system 166-Mev $O^{16}+U^{238}$. ψ_1 at 90 deg. Each arrow represents the estimated peak position for the capture of the indicated fragment from the incident heavy ion.

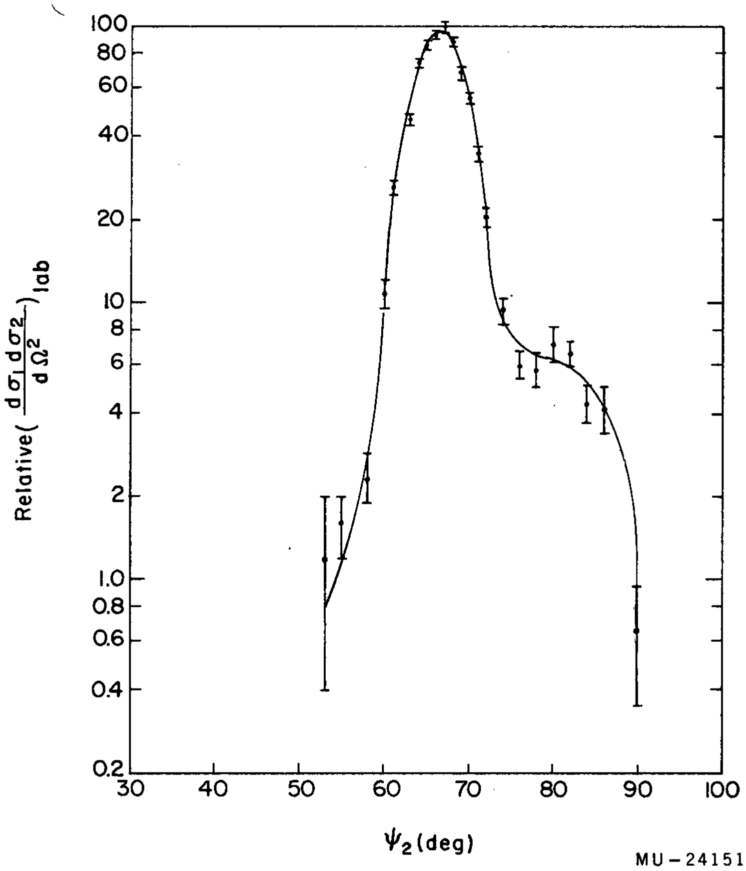

Fig. 7. Fission-fragment angular correlation for the system 140-Mev $O^{16}+U^{238}$. ψ_1 at 90 deg.

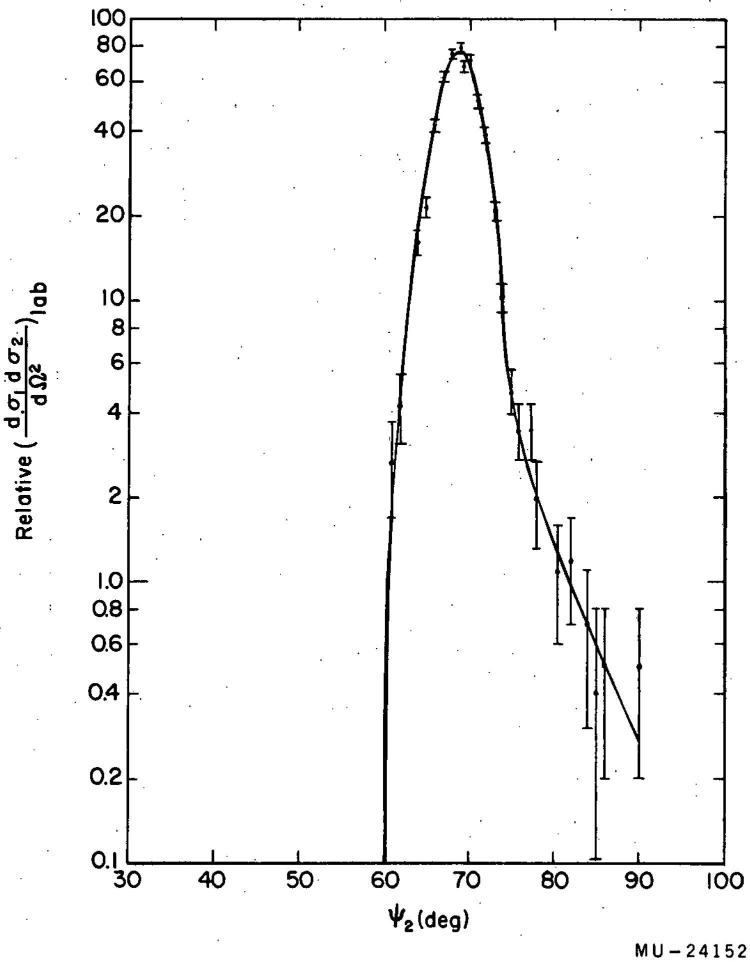

Fig. 8. Fission-fragment angular correlation for the system 110-Mev $O^{16}+U^{238}$. ψ_1 at 90 deg.

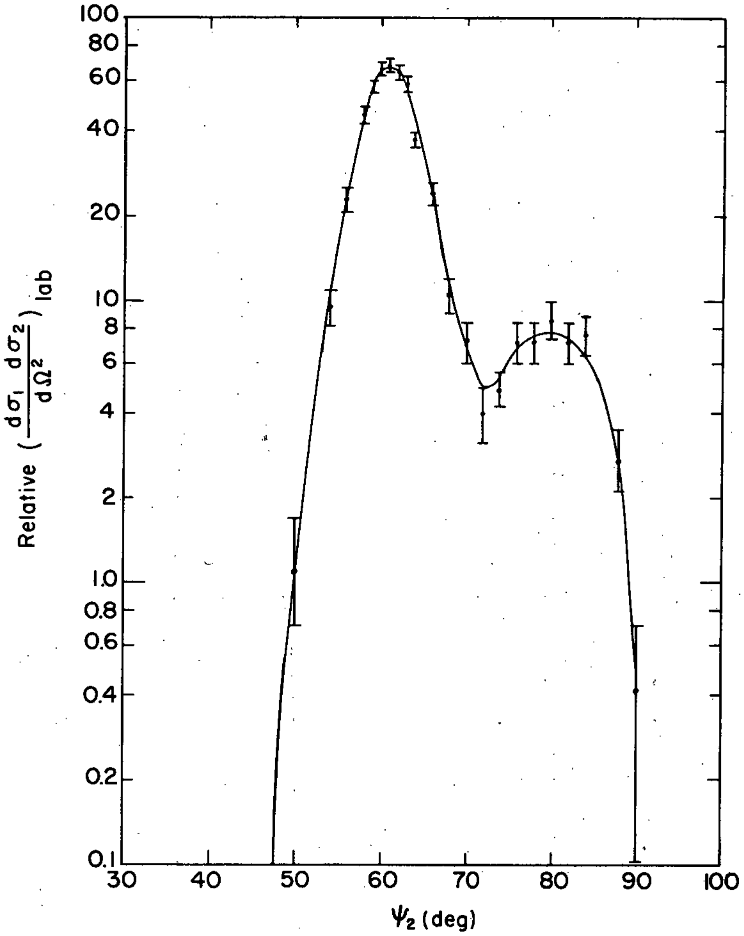

MU-24153

Fig. 9. Fission-fragment angular correlation for the system 207-Mev $Ne^{20}+U^{238}$. ψ_1 at 90 deg.

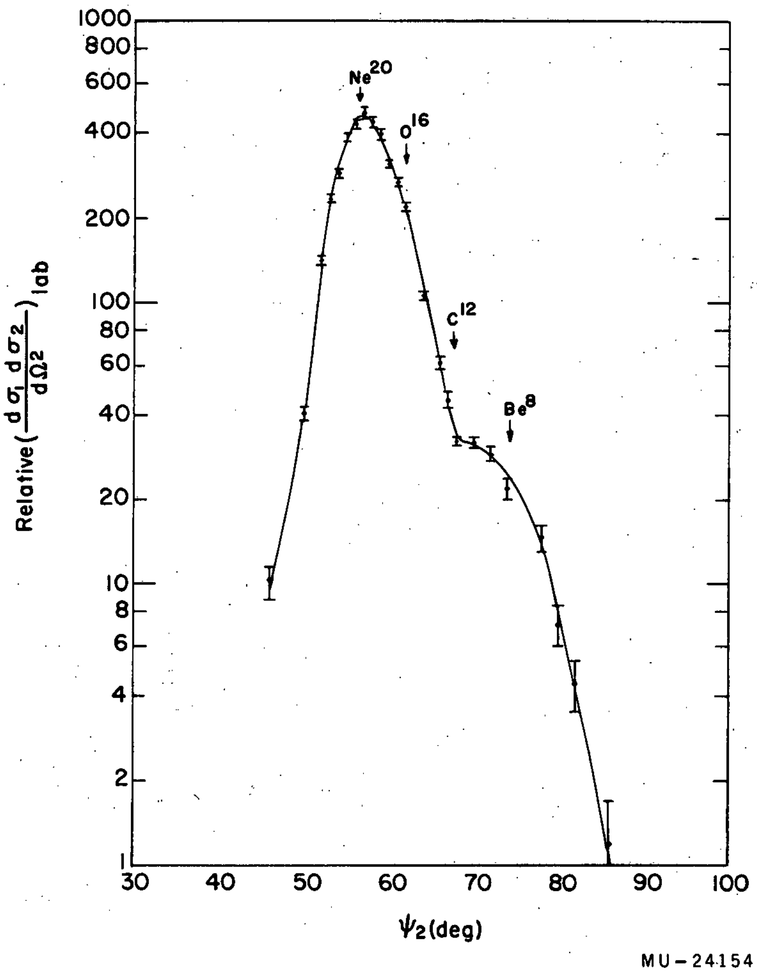

Fig. 10. Fission-fragment angular correlation for the system 207-Mev Ne^{20}+Bi^{209}. ψ_1 at 90 deg. Each arrow represents the estimated peak position for the capture of the indicated fragment from the incident heavy ion.

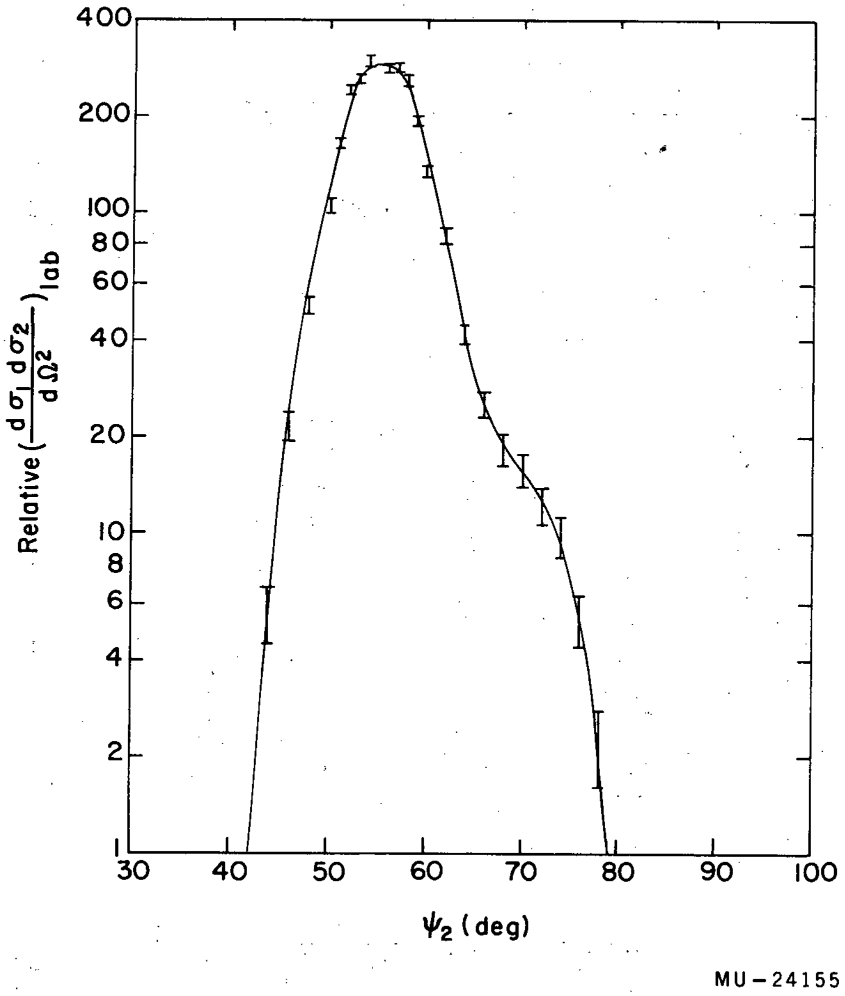

Fig. 11. Fission-fragment angular correlation for the system 207-Mev $Ne^{20}+Au^{197}$. ψ_1 at 90 deg.

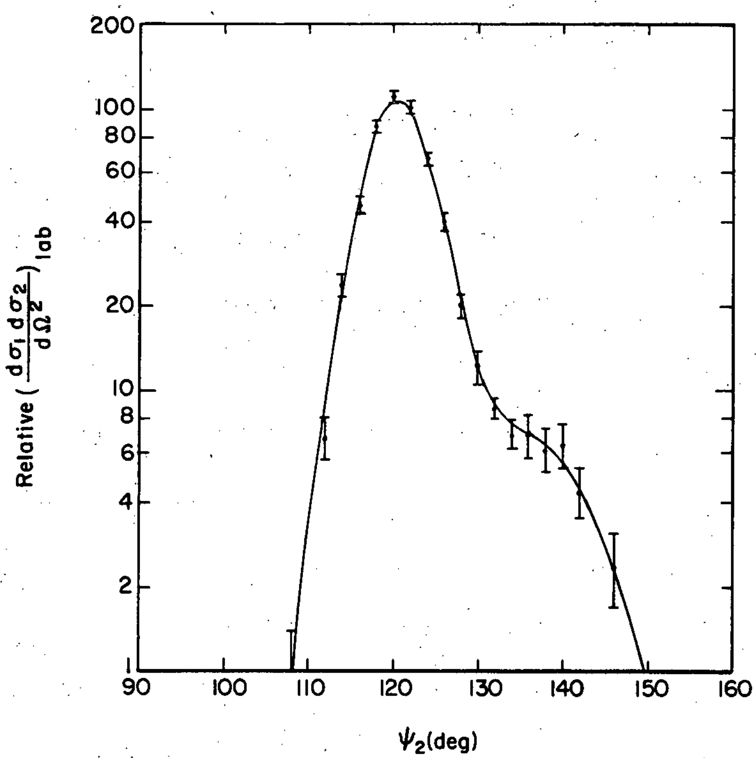

Fig. 12. Fission-fragment angular correlation for the system 166-Mev $O^{16}+U^{238}$ ψ_1 at 40 deg.

In the following we compare the experimentally determined x_{mp}^2 with estimated most probable values, $\bar{x}_{CN}^2$. For such a reaction, assuming the particles emitted before fission are evaporated, $\bar{x}_{CN}^2$, for a CN is given by

$$\bar{x}_{CN}^2 = \frac{A_I \cdot E_I \cdot A_{ff}}{A_{CN}^2 \cdot E_{c.m.}} , \qquad (5)$$

where A_I is the mass and E_I the lab kinetic energy of the heavy ion; A_{CN} is the mass of the compound nucleus; A_{ff} and $E_{c.m.}$ are as defined before. Because the prompt neutrons emitted in the fission process presumably are isotropic in the framework of the fragments, final values for A_{ff} and $E_{c.m.}$ can be used. Values for $E_{c.m.}$ after prompt neutron emission, for some of the systems studied here, have been measured by several groups.[1,2,10] In cases in which no data were available, energy measurements were carried out as shown under "Energy Measurements". $E_{c.m.}$ is known to within 4%. A_{ff} was estimated by assuming a symmetric division. We then have $A_{ff} = 1/2\ (A_{fN} - \bar{\nu})$ where A_{fN} is the mass of the fissioning nucleus and $\bar{\nu}$ the mean number of neutrons emitted in the fission process; $\bar{\nu}$ is estimated from Leachman's relationship,[11]

$$\bar{\nu} = \bar{\nu}_o + 0.12\ E, \qquad (6)$$

where E is the excitation energy of the fissioning nucleus and $\bar{\nu}_o$ the mean number of neutrons emitted in spontaneous fission. The $\bar{\nu}_o$ varies with Z and A in a systematic manner. Values for $\bar{\nu}_o$ were taken from the compilations by Huizenga and Vandenbosch.[12] Early in the evaporation chain, the fissioning nucleus has a higher mass but also a higher excitation energy, which results in emission of a larger number of neutrons in the fission process than later in the chain. A_{ff} therefore shows a small variation along the chain. The calculated values given in Table I are averages for the whole chain. Experimental values exist only for the system Au + 114-Mev C^{12}. Blann gives the value 97.5±2.5 for A_{ff},[13] which is to be compared to the estimated value of 98.5. This, then, gives an idea of the errors involved. The over-all uncertainty in the calculated values for x_{CN}^2 given in Table I is of the order of 5%. The agreement between x_{mp}^2 and $\bar{x}_{CN}^2$ is therefore to be regarded as satisfactory. The CN reaction thus is the most probable event for both groups.

It is reasonable to assume that the CN reactions in Group II should give symmetric coincidence curves similar to those in Group I. We further assume that towards lower angles of the peak (at higher x^2 values), the events are coming from CN reactions. We have accordingly constructed complete CN curves. These curves also have half-widths of about 6 to 8 deg. A curve representing NCN reactions is then obtained by subtracting the total CN curve from the total coincidence curve. This is shown for the $O^{16} + U^{238}$ system in Fig. 6. The percent contributions from NCN reactions to the total fission cross section were obtained by integrating the area of both the CN and the NCN contributions and are given in Table I. It appears that in all cases most of the events proceed as CN reactions. The ratio for the NCN reaction is lower at 40 deg than at 90 deg, indicating a more nearly isotropic distribution of the fragments from this reaction. This is to be expected because the angular momentum deposited is less than for a CN reaction.[2]

The numbers given must be regarded, however, as only roughly approximate. The most serious uncertainty is due to insensitivity of the method to separate reactions that have small differences in momentum transfer. We see, for instance, in U^{238} that close to the CN peak any small contribution from NCN reactions is not detectable. In particular, the reaction between U^{238} and 73-Mev C^{12} has been classified as 100% CN reaction, although spallation studies have shown that even at this energy there is contribution from NCN reactions.[14] The method is, however, useful as a tool for the study of reactions with large differences in x^2, which might occur in heavy-ion bombardments.

In the following we discuss possible reaction mechanisms that can contribute to the NCN peak.

Spallation products from reactions which can be written as (C^{12}, Be^{8} xn), (N^{14}, B^{10} xn) and (O^{16}, C^{12} xn) have been observed with high yields.[15] Similarly products from reactions such as (HI, αxn) and (HI, pxn), with the first one dominating, have been observed although with less frequency.[16] Britt and Quinton have directly observed alpha particles, protons and heavier fragments and found them to be peaked in the forward hemisphere.[17] The α's and p's were found to have velocities close to the velocity of the incoming heavy ion. The frequency of direct-interaction alphas was about three times that of protons. An interesting observation made by the same group was that the number of α particles was higher in bombardment with C^{12} ions than with N^{14} or O^{16}. These α particles could arise from the reaction (C^{12}, Be^{8}) followed by the disintegration of Be^{8} into two α particles.

Using this information, we have indicated possible reactions that could account for the NCN curve demonstrated in Figs. 6 (O^{16} + U^{238}) and 10 (Ne^{20} + Bi^{209}). We have assumed that for these reactions, symmetric fission is the most probable event. For the different types of reactions x_{mp}^{2} can then be calculated if the stripped ion continues forward with the same velocity as the incoming ion.

It appears that reactions involving the transfer of one α particle are not observed for the reactions with Ne^{20} incident on Au and Bi targets. Such reactions do not deposit high enough excitation energy in the residual nucleus for it to undergo fission, because the fission threshold is so high that the level width for fission is too low to allow fission to be detected. However, the transfer of larger fragments can contribute a substantial amount of fission, as is indicated in the curves.

For U^{238}, on the other hand, a significant component of the α-particle transfer reaction is observed. We now discuss the NCN curve for U^{238} and 166-Mev O^{16} in more detail. The observed peak position corresponds to transfer of 30% of the forward momentum of the heavy ion. This is to be compared with 25% for α-particle transfer if the fissioning nucleus continues in the direction of the beam axis. Apparently the emitted particles exchange some of their momenta with the struck nucleus.

We notice further that the half-width of the peak is larger than expected at this low x^2 value. Possible explanations for this are:

(a) a wide spread in the momentum of the fissioning nucleus,

(b) an admixture of other transfer reactions,

(c) internal motion of the nucleons in the O^{16}.

Another interesting observation is that fission-fission coincidences are recorded with the detectors 180 deg apart even after corrections have been made for the angular spread of the detectors. The following factors contribute to this apparent "negative" momentum transfer:

(a) internal motion of the nucleons in the O^{16},

(b) evaporation of neutrons from the fission fragments,

(c) admixture of reactions with small momentum transfer, such as n and p nucleon transfer and Coulomb excitation,

(d) scattering in the target and backing. (Comparison of 750-μg/cm^2 and 250-μg/cm^2 targets indicates that this effect is negligible.)

The presence of transfer reactions was confirmed in the following way. The dominant α-particle transfer reaction can be written U^{238} $(O^{16}, C^{12})Pu^{242*}$, whereas the CN reaction is U^{238} (O^{16}) Fm^{254*}. These two nuclei decay predominantly by fission. Since neutron evaporation dominates over charged-particle evaporation,[17,18] we should expect the fragments that enter the detectors when the system is at the CN peak to be coming from fissioning Fm isotopes.

Similarly, at the NCN peak, we should see fission from Pu isotopes. One detector was first fixed at 64.5 deg with geometry corresponding to the peak for the CN reaction, and the energy spectrum of the coincident fragments was observed in the other detector - at 90 deg. The most probable energy was found to be 93 Mev (c.m.). The first detector was then set at 81.5 deg and the most probable kinetic c.m. energy of the fragments entering the detector at 90 deg was found to be 85.5 Mev. These are reasonable values for the elements in question.

It is interesting to note that the same procedure can be used to measure the angular distribution of the fragments from the CN reactions. By adjusting the relative positions of the two detectors, one can practically exclude fragments originating in undesired reactions from entering the detectors.

CONCLUSION

The method used in this investigation is useful for measuring directly and with a high degree of accuracy the x_{mp}^2 values for reactions leading to fission. Estimated x_{CN}^2 values agree very well with the x_{mp}^2 measured for several combinations of targets and heavy ions. The dominant reaction appears to be one in which the heavy ion deposits its full momentum. Evidence is also presented for reactions with incomplete momentum transfer. We have estimated the relative amounts of these NCN reactions contributing to fission. For Ne^{20} + Au^{197} and Ne^{20} + Bi^{209} large fractions of the momentum, corresponding to eight or more nucleons, are transferred. With a U^{238} target the dominant NCN reaction is an α-particle transfer reaction. The momentum of the fissioning nucleus in this case has a wider spread than the momentum of the nucleus in a CN reaction and its most probable momentum is higher than 1/4 of the momentum of the O^{16} ion.

ACKNOWLEDGMENTS

The excellent design of the chamber was done by Charles A. Corum. We are very thankful for the help of Almon E. Larsh, Leonard E. Gibson, and William W. Goldsworthy with the electronics. Robert Latimer furnished us with the indispensable silicon detectors. We are grateful to the Hilac crew for the good beams of ions through many hours of running time. Daniel G. O'Connell was most helpful in preparing some of the targets used in the experiments.

REFERENCES

1. G. E. Gordon, A. E. Larsh, T. Sikkeland, and G. T. Seaborg, Phys. Rev. 120, 1341 (1960).

2. T. Sikkeland, A. E. Larsh, and G. E. Gordon, Fission of Uranium-238 with Carbon Ions, Phys. Rev. (to be published).

3. Victor E. Viola, Jr., Angular Distributions from Heavy-Ion-Induced Fission (Thesis), UCRL-9619, March 1961.

4. E. Goldberg, H. L. Reynolds, and D. D. Kerlee, in Proceedings of the Second Conference on Reactions between Complex Nuclei (John Wiley and Sons, Inc., New York, 1960) p. 230.

5. J. M. Alexander and M. F. Gazdik, in Chemistry Division Annual Report for 1960, UCRL-9566, Feb. 1961, p. 145.

6. E. L. Hubbard, W. R. Baker, K. W. Ehlers, et al., Heavy-Ion Linear Accelerator, UCRL-9453, Nov. 1960.

7. L. C. Northcliffe, Phys. Rev. 120, 1744 (1960).

8. Robert M. Latimer (Lawrence Radiation Laboratory), unpublished work, 1961.

9. J. S. Fraser and J.C.D. Milton, in Proceedings of the Second United Nations International Conference on the Peaceful Uses of Atomic Energy, Geneva, 1958 (United Nations, New York, 1958), Vol. 15, p. 216.

10. H. C. Britt and A. R. Quinton, Phys. Rev. 120, 1768 (1960).

11. R. B. Leachman, in Proceedings of the Second International Conference on the Peaceful Uses of Atomic Energy, Geneva, 1958 (United Nations, New York, 1958) Vol. 15, p. 229.

12. J. R. Huizenga and R. Vandenbosch, Nuclear Fission, to be published in Nuclear Reactions, Vol. 2 (North-Holland Publishing Co., Amsterdam, Netherlands).

13. H. Marshall Blann, Fission of Gold with 112-Mev C^{12} Ions: A Yield-Mass and Charge-Distribution Study (Thesis), UCRL-9190, May 23, 1960.

REFERENCES (Con't)

14. T. Sikkeland, S. G. Thompson, and A. Ghiorso, Phys. Rev. 112, 543 (1958).

15. A. Ghiorso and T. Sikkeland, in Proceedings of the Second Conference on the Peaceful Uses of Atomic Energy, Geneva, 1958 (United Nations, New York, 1958) Vol. 14, p. 158.

16. A. Ghiorso, T. Sikkeland, A. E. Larsh, and R. M. Latimer (Lawrence Radiation Laboratory), unpublished work.

17. H. C. Britt and A. R. Quinton, Alpha Particles and Protons Emitted in the Bombardment of Au^{197} and Bi^{209} by C^{12}, N^{14}, and O^{16} Projectiles, Phys. Rev. (to be published).

18. E. Hubbard, R. Main, and R. Pyle, Phys. Rev. 118, 507 (1960).